Nano-crystals of Cerium-Hafnium Binary Oxide: Their Size-dependent Structure

Joan M. Raitano, Syed Khalid, Nebojsa Marinkovic, Siu-Wai Chan

PII: S0925-8388(15)01359-6
DOI: http://dx.doi.org/10.1016/j.jallcom.2015.05.066
Reference: JALCOM 34182

To appear in: *Journal of Alloys and Compounds*

Received Date: 3 March 2015
Revised Date: 25 April 2015
Accepted Date: 10 May 2015

Please cite this article as: J.M. Raitano, S. Khalid, N. Marinkovic, S-W. Chan, Nano-crystals of Cerium-Hafnium Binary Oxide: Their Size-dependent Structure, *Journal of Alloys and Compounds* (2015), doi: http://dx.doi.org/10.1016/j.jallcom.2015.05.066

Nano-crystals of Cerium-Hafnium Binary Oxide: Their Size-dependent Structure

Joan M. Raitano[a*], Syed Khalid[b], Nebojsa Marinkovic[c], Siu-Wai Chan[a]

[a]*Department of Applied Physics and Applied Mathematics, Materials Science and Engineering Program, Columbia University, New York, New York 10027, USA*

[b]*National Synchrotron Light Source, Brookhaven National Laboratory, Upton, New York 11973, USA*

[c] *Chemical Engineering Department, Columbia University, 500 W 120th St, Mudd 801, New York,NY 10027, USA*

**joanraitano@gmail.com, 516-884-4105*

Abstract

Cerium oxide (CeO_2, "ceria") and hafnium oxide (HfO_2, "hafnia") were aqueously co-precipitated and subsequently calcined to allow for homogenization. The size of the $(1-x)CeO_2$-$xHfO_2$ crystallites, determined by the Scherrer equation, varied from 140 nm for x=0 to 15 nm for x =0.73. For $x \leq 0.14$, only cubic structures are visible in x-ray diffractograms, and the lattice parameters are consistent with the values expected for structurally cubic solid solutions of hafnia in ceria. At x=0.26, tetragonal and monoclinic phases nucleated with the former not being observed in the bulk phase diagram for ceria-hafnia. Therefore, the solubility limit of the cubic structure is between x=0.14 and x = 0.26 for 40 nm to 61 nm crystallites, the sizes of these respective compositions. More specifically, for the 40 nm crystallites of x=0.26 $(1-x)CeO_2$-$xHfO_2$, 15% of the hafnia remains in a structurally cubic solid solution with ceria based on the observed cubic lattice parameter. The compositional domain for the cubic fluorite structure in this study is narrower than other nanostructured $(1-x)CeO_2$-$xHfO_2$ studies, especially studies with crystallite sizes less than 10 nm, but wider than observed in the bulk and helps to expand the size regime over which the relationship between crystallite size and phase stability is known. The extent of this cubic-structure domain is mainly attributable to the intermediate crystallite size and the roughly zero Ce^{3+} content as determined by x-ray absorption near edge structure spectroscopy.

Keywords

Nanostructured materials; Oxide materials; Crystal structure; Synchrotron radiation; X-ray diffraction

1. Introduction

Interest in applications combining hafnium oxide (HfO_2, "hafnia") and cerium oxide (CeO_2, "ceria") has increased in recent years. A solid solution of ceria and hafnia has been used as the heart of an oxygen sensor[1]. In catalysis, ceria-hafnia solid solutions have been found to be useful in soot oxidation[2], CO oxidation[3], and dehydration of an alcohol[4]. In microelectronics, alternating layers of the two oxides have been employed as a potential gate dielectric because hafnia's high dielectric constant reduces the leakage current, while ceria acts to passivate germanium in Ge-based devices[5].

Previous studies on the structure of ceria-hafnia solid solutions can be divided into thin film studies and powder studies. Thin film studies[6, 7] will not be considered here as they can be influenced by lattice mismatch with the substrate and by near-vacuum deposition conditions in which nano-ceria would be very susceptible to reduction[8]. Powder studies that consider phase stability for 10% or less hafnia in ceria[9, 10] or that employ an additional metal beside

cerium and hafnium[11] will not be considered. Table 1 is a list of ceria-hafnia powder studies including the extent of the structurally cubic domain as well as the method of preparation and crystallite size where provided. The column headed by "Sample reduced" indicates whether there is information presented in the article regarding oxygen deficiency in the samples prior to any temperature-programmed reduction or other reduction procedures. Finally, the column headed by "Checked lattice parameter" indicates if the authors explicitly mentioned checking the lattice parameter to see if it was consistent with a single phase, structurally cubic solid solution with the specified ceria-hafnia ratio.

Table 1: Non-film studies (pellets and "free crystallites")

Reference	**Method**	**cubic crystallite size (nm)**	**Cubic domain: *x* in (1-*x*) CeO_2-*x*HfO_2**	**Sample reduced**	**Checked lattice parameter**
Debray, et al.[12]			0-0.12		
Chavan, et al.[13]	Physical mixing & heating		0-0.15		yes
Reddy, et al. [14]	CP & anneal	4.6-13.1	0-0.20		yes
Passerini, et al.[15]	CP & anneal		0-0.32		yes
Gavrish, et al.[16] ⊗	Physical mixing & roasting	μm	0-0.425	likely	
Baidya, et al. [17]	Solution combust-ion	7 *	0-0.50		
Zhou, et al.[18]	Sol-gel	7-8	0-0.50		yes

⊗ pellet study

* This value is not found in the paper. It is an estimate based on the XRD data presented.

According to the stable lines in the bulk ceria-hafnia phase diagram[16], the solubility of hafnia in the cubic fluorite structure with ceria is less than 5%. The metastable solubility limit for hafnia in a cubic solid solution with ceria, (1-*x*)CeO_2-*x*HfO_2, varies including low values of

x=0.12 reported by Debray, et al.[12] and x=0.15 reported by Chavan, et al[13]. Reddy, et al.[14] and Passerini, et al.[15] report pure structurally cubic ceria-hafnia solid solutions with x =0.2, and 0.32, respectively, but only Passerini, et al.[15], indicates that this is a solubility limit. In these two studies, the ceria-hafnia powders were prepared by co-precipitation and subsequent calcination as is the case in the work being presented here. Greater solubility of hafnia in a structurally cubic solid solution with ceria was reported in Gavrish, et al[19]. In this study, ceria and hafnia were physically mixed and then calcined at temperatures of 1500°C or higher. Finally, the highest solubility, x=0.50, was reported in Baidya, et al.[17], and Zhou, et al.[18]. The powders in these studies were prepared by solution combustion and sol-gel processing, respectively.

The aforementioned articles provide useful information regarding ceria-hafnia solid solutions, but do not provide a complete picture for a few reasons. First, some of the articles do not provide crystallite size information [12, 15, 16]. Second, those that do provide size information are either really small (less than or equal to 13 nm)[17, 18] or very large (micron-sized)[19]. Research in the twin[20] system, zirconium oxide (ZrO_2, "zirconia") combined with ceria, has clearly demonstrated that reduced crystallite size can greatly enhance the structural stability of the cubic fluorite phase[21]. Third, although at least one of these articles studies the reduction of ceria-hafnia[17], it is not completely clear what the concentration of Ce^{3+} is in the samples after calcination, but before reduction. This is a relevant factor as the presence of Ce^{3+} has been shown to greatly enhance the phase stability of the cubic fluorite structure[22].

2. Experimental procedures

Precursors of hafnia-doped cerium oxide were prepared by mixing a solution of $HfOCl_2 \bullet 8H_20$ (Alfa Aesar 99.998%) and $Ce(NO_3)_3 \bullet 6H_20$ (Alfa Aesar, 99.5%), having a total cation concentration of 0.04M (i.e., Ce^{4+} + Hf^{4+}), with a 0.5 M hexamethylenetetramine ($(CH_2)_6N_4$, also known as "HMT", Alfa Aesar, 99+%) solution at room temperature. After centrifugation, the precipitates, which were composed of ceria nanocrystallites and amorphous hafnia, were dried under ambient conditions. The concentration of cerium and hafnium in the products was determined by inductively coupled plasma-atomic emission spectroscopy (ICP-AES) analysis (Desert Analytics, Tucson, Arizona, now known as Columbia Analytics).

To determine the minimum temperature for sample homogenization, portions of the 88%CeO_2-12%HfO_2 sample were calcined at temperatures from 350 to 1250°C, and the lattice parameters of the resulting powders were determined. For each calcination, a ramping rate of 6.8°C/min was used with a hold at the maximum temperature for 15 minutes. After the hold, the power to the furnace was cut and the samples were removed. Once the minimum temperature was determined, further calcinations were conducted nominally at 1050ºC or 1250°C. When more than one sample was calcined at a time, as was the case sometimes for the 1250ºC calcinations, a slight displacement from the furnace center meant the maximum temperature could have been as low as 1180°C.

X-ray diffraction (XRD) measurements were made using an Inel 3000 diffractometer (Artenay, France) equipped with a position sensitive detector (PSD) and a copper target. Diffractograms were collected through a two theta (2θ) value of roughly 100°, although only a portion of this data will be shown in the figures below. The resulting files were converted from text to the .cpi format using ConvX[23]. Then the files were fitted using XFit[24] with the CuKa_5.lam emission profile, which was found to produce the best fits of the data. Experimental

diffraction results were compared to International Centre for Diffraction Data (I.C.D.D.) standards for pure ceria and the polymorphs of hafnia in order to identify the phases present.

Crystallite size calculations for the cubic structure, based on XRD data, were done using the Scherrer equation, $d = K\lambda/B\cos\theta_B$, where d is the crystallite size, λ is the wavelength, B is the FWHM of the Bragg peak corrected for instrumental broadening, θ_B is the Bragg angle, and K is the Scherrer constant with a value of 0.9[25]. More specifically, the crystallite sizes of the cubic fluorite structures were calculated using the (111) XRD peak because the lowest 2θ peak is least affected by strain-broadening[24]. Also of note are two additional items. First, an alumina (Al_2O_3) plate having micron-sized grains (NIST Standard Reference Material® 1976) was used for the instrumental correction. More specifically, the (012) Al_2O_3 peak was used for the aforementioned correction because its angular position (roughly 26° with CuKα radiation) was closest to that of the first peak of the (1-x)CeO_2-$x$$HfO_2$ samples (roughly 29° with CuKα radiation). Second, the crystallite size for the pure hafnia sample provided below is an approximation[26] in that the same value of the Scherrer constant is used (i.e., 0.9), although the shape of monoclinic hafnia tends to be rod-like (cylindrical)[27].

Many of the XRD measurements made in this study were collected with the powder on a glass slide, rather than a recessed holder; therefore, there is reason to suspect that the accuracy of the lattice parameter results will compromised by physical displacement errors. With PSD-XRD instruments like the one used here, Pramanick, et al.[28], has shown by geometrical arguments and experimental results that such displacement errors, resulting from the positioning of the sample, can be expressed as

$$\Delta d/d = -K\cos^2\theta_B \qquad (1)$$

where K is a constant, d is the plane spacing, and Δd is the error in plane spacing. Then the authors showed how an accurate value of the lattice parameter could be determined, even with substantial sample displacement, by plotting the lattice parameter, a, calculated for each Bragg angle, as a function of $\cos^2\theta_B$ and extrapolating to the y axis (where $a = a_o$ or the calculated lattice parameter for each peak, a, approaches the true lattice parameter, a_o)[28].

The Cohen method[29, 30] for determining a_o is reputed to minimize random errors[24] in XRD data. Combining the Pramanick, et al.[28], extrapolation function (equation (1)) with the Bragg equation, the proper expression for the Cohen method results [25]:

$$\sin^2\theta = C\alpha + A\delta \qquad (2)$$

where C and A are unknowns, and α and δ are defined in the following manner:

$$\alpha = h^2+k^2+l^2 \qquad (3)$$

$$\delta = 10\sin^2 2\theta \qquad (4)$$

and where h, k, and l are the indices of the planes corresponding to each of the diffraction peaks at θ_B. The values of C and A are determined by performing a multiple regression in which α and δ are the independent variables, $\sin^2\theta$ is the dependent variable, and the intercept is set to zero. Finally, a_o is calculated by knowing that

$$C = \lambda^2/4a_o^2 \qquad (5)$$

where λ=wavelength of diffractometer radiation being used in the analysis. The derivation of equation (2) has been done in detail elsewhere for the error in Debye-Scherrer camera data ($\Delta d/d$), which is also proportional to $K\cos^2\theta_B$ coincidentally[25]. Note also that the lowest 2θ cubic fluorite peaks, (111), (200), and (220), were not used in these fits as the error in $\sin\theta$ tends to decrease as the value of θ increases[24].

The expected lattice parameter of a cubic solid solution of hafnia in ceria can be predicted based on an empirical formula determined by Kim[31]. For a single dopant (i.e., HfO_2) in CeO_2 and a common oxidation state for the host and the dopant metal (i.e., 4+ for both cerium and hafnium cations), the equation can be expressed as the following:

$$a_{o,Ce} = 0.5413 + 0.0220\Delta r(m_d) \quad (6)$$

where $a_{o,Ce}$ is the lattice parameter of doped ceria (in nm) at room temperature, Δr is the difference in ionic radius (nm) between the dopant and host cations in eightfold coordination from Shannon[32], and m_d is the mole percent of the dopant.

X-ray absorption near edge structure (XANES) spectroscopy was performed at beamline X19A at Brookhaven National Laboratory's National Synchrotron Light Source (BNL's-NSLS) to characterize the oxidation state of cerium in the $(1\text{-}x)CeO_2\text{-}xHfO_2$ crystallites. Measurements were made at the Ce LIII edge with an energy step size of 0.2 eV and a monochromator settling time of 0.5 seconds in the 30 eV before and after the absorption edge. The oxidation state standard for Ce^{4+} was micron-sized crystallites of CeO_2 (99.99%, Alfa Aesar); the Ce^{3+} standard was Ce_2S_3 (99.9%, Alfa Aesar). Linear combination fitting of these standards to the nanostructured ceria-hafnia samples was done with Athena software[33].

3. Results

Some ceria-hafnia nano-crystals considered below are solid solutions of CeO_2 and HfO_2 and could be described as $Ce_{1-x}Hf_xO_2$ where x = 0 to 1. However, since other samples will consist of more than one phase and thus actually be a mixture of different solid solutions, samples will be indicated as $(1\text{-}x)CeO_2\text{-}xHfO_2$ generally.

In Table 2, the mole fraction (x) of Hf^{4+} present in the initial solution of $HfOCl_2 \bullet 8H_2O$, and $Ce(NO_3)_3 \bullet 6H_2O$ ($Hf^{4+}/(Hf^{4+}+Ce^{3+})$) is provided along with the mole fraction of Hf^{4+} in the final crystallites as determined by ICP-AES.

Table 2: Sample composition and concentration of Ce^{3+}

x in $(1\text{-}x)CeO_2\text{-}xHfO_2$ aqueous precursor	**x in $(1\text{-}x)CeO_2\text{-}xHfO_2$ solid product***	***cubic* crystallite size (nm)≠**	**[Ce^{3+}] by XANES**
0	0	140±20	--
0.016	0.037	74±3	0
0.033	0.14	61±2	0
0.090	0.26	40±1	0
0.099	0.47	35±1	0
0.270	0.73	15±1	--
1	1	53±6 γ	--

* All values determined by ICP-AES except x=0 and x=1.

≠ Determined by applying the Scherrer equation to the first XRD peak.

γ Estimation of the monoclinic structure crystallite size as described in the experimental section

The minimum temperature for complete homogenization of samples in air was determined by room temperature x-ray diffraction measurements to be 1050°C (Fig. 1). As can be seen in the figure, the lattice parameter decreases as the dwell temperature increased up to 1050°C. This decrease in lattice parameter (a_o) is anticipated as the oxides become homogeneous and hafnia crystallizes because the ionic radii of Ce^{4+} and Hf^{4+} are 0.97Å, and 0.83Å (in eightfold coordination), respectively[25]. That is, the pre-calcination sample contains crystalline ceria and amorphous hafnia, and the fluorite lattice shrinks as hafnia becomes a part

of the lattice. Moreover, the value of a_o at 1050°C is close to the expected value for a $0.88CeO_2$-$0.12HfO_2$ solid solution as predicted by equation (6). Note that this expected lattice parameter is indicated by the horizontal dotted line in the figure. Furthermore, the overall trend observed in Fig. 1, which shows the a_o values calculated with the Cohen method, is the same if the Cohen method is not used, and a_o is more simply obtained from the intercept[28] of the plot of a, the lattice parameter calculated for each peak, as a function of $\cos^2\theta$ (this alternate version of Fig. 1 not shown).

The x-ray diffraction data for samples annealed in air at a nominal temperature of 1250°C for 15 minutes are provided in Fig. 2a; the high 2θ data is not shown because the peaks are too weak to be visible on the scale of the image. Comparing this data to that of the ICDD standards (Fig. 2b), it is apparent that the ceria-rich samples in this figure, from x=0 to x =0.14, are cubic (c), exhibiting the characteristic peaks of the fluorite structure (PDF 00-034-0394)[34]. For x= 0.26, the structure is predominantly cubic with very weak monoclinic (m) (PDF 04-005-4477)[35] and possibly tetragonal (t) (PDF 04-002-5486)[34] peaks, not visible on the scale of the figure, and so labeled c* to distinguish it from the pure cubic structure phase. For x =0.47, a mixture of cubic and monoclinic structures are evident, but, for x = 0.73, besides the cubic and monoclinic peaks, another peak is present that may again be attributable to the tetragonal structure and is labeled with a "t". Finally pure hafnia displays a monoclinic structure.

Fig. 3 presents a closer view of some of the XRD data between 27 and 35º because ceria and the tetragonal and monoclinic polymorphs of hafnia have their most intense peaks in this 2θ domain as is evident in Fig. 2b. In the figure, from x =0 to x = 0.14, the structure is cubic. Moreover, as the hafnia content increases from x=0 to x =0.14, the lattice parameter decreases and is roughly consistent with the expected lattice parameter of structurally cubic ceria-hafnia solid solutions [31] as indicated by the dotted line (Fig. 4). For x=0.26, the structure is mainly cubic with slight noncubic peaks mentioned above. These weak monoclinic and tetragonal peaks are barely evident on the scale of Fig. 3, but when we consider the lattice parameter of this composition (Fig. 4), we see that the value is very close to that of x = 0.14 and not consistent with the dotted line indicating the expected cubic lattice parameter for x = 0.26. In fact, based on the lattice parameter exhibited by this sample, 5.366Å, the hafnia content in a cubic fluorite solid solution with ceria can be estimated to be 15% for these 40 nm crystallites. For x=0.47, the monoclinic peaks become prominent in XRD, and the lattice parameter remains far above the dotted line.

Two other points have been added to Fig. 4 from Fig. 1. These belong to the x=0.12 (1-x)CeO_2-$x$$HfO_2$ samples calcined at 1250ºC and 1050ºC. Both samples showed only cubic fluorite peaks in the XRD data, and while the lattice parameter for the 1250ºC is slightly above the aforementioned expected a_o line, it is within the error limit.

Crystallite size of the *cubic structure* decreased as the hafnia content increased from x =0 to x =0.73 in (1-x)CeO_2-$x$$HfO_2$ (Table 2). The crystallites are largest at the two terminal compositions 140 nm (CeO_2) and 53nm (HfO_2). The smallest are only 15 nm ($0.73\ HfO_2$-$0.27CeO_2$) showing HfO_2-addition is an effective anti-coarsening agent.

By visual inspection, it can be seen that the XANES spectra for nanostructured ceria-hafnia (Fig. 5) are very similar, in shape and absorption edge position, to the spectrum for pure micron-sized CeO_2. Linear combination fitting with micron CeO_2 as the Ce^{4+} standard and Ce_2S_3 as the Ce^{3+} standard shows that the Ce^{3+} concentration is approximately zero in all of the (1-x)CeO_2-$x$$HfO_2$ crystallites tested (Table 2).

4. Discussion

In this study, the mole fractions of hafnia collected by centrifugation and subsequently tested by ICP-AES are greater than those originally measured out as reactants (Table 2). This enrichment in hafnia content in the product relative to the precursor is likely explained by differences in the kinetics of hafnia and ceria precipitation. By visual examination during the preparation of hafnia, it is evident that the precipitation is almost immediate. Such an immediate reaction is not seen during ceria preparation, and research has shown that the volume of ceria nanoparticles increases steadily over the course of roughly 12 hours at cerium nitrate and HMT concentrations similar to those used in this study[36].

With calcination at 1050°C or higher for fifteen minutes, these co-precipitated oxides became homogenized (Fig. 1). Requiring such a high temperature is not surprising as cation size differences, as exist between Ce^{4+} and Hf^{4+}, have been shown to hinder diffusion, and the extent of the hindrance increases as the radii[37] difference increases. The slight downward displacement of the lattice parameter for the x=0.04 sample calcined at 1250ºC (Fig. 4) and the x=0.12 sample calcined at 1050ºC (Fig. 1 and Fig. 4) with respect to the expected lattice parameter (dotted line), may be due to the Kim[31] article using a lattice parameter of 5.413Å for pure ceria, while the pure ceria in this study displayed a slightly smaller a_o value (Fig. 4).

The solubility limit of hafnia in ceria is somewhere between x=0.14 and x=0.26 for 40 to 61 nm $(1-x)CeO_2$-$xHfO_2$, the crystallite sizes of these respective compositions. This limit is made evident by the intrusion of the strongest monoclinic peak in the x=0.26 sample (Fig 3). The solubility limit is also signaled by the cubic lattice parameter reaching its lowest value at either the x=0.14 or x=0.26 composition for the samples calcined at 1250ºC (Fig. 4). (The error in the lattice parameter, a_o, makes it unclear which one is truly the lowest.) However, it is clear that the limit is much closer to x=0.14, than 0.26, since the lattice parameter for x=0.26 roughly remains at the expected a_o for x=0.14. In keeping with the idea that the solubility limit is close to x=0.14, the hafnia content in a structurally cubic solid solution with ceria for this x=0.26 sample was calculated to be 15% using equation (6). This limit may hold for the 35 nm x=0.47 ceria-hafnia crystallites as well, but this is a rough approximation given the uncertainty in the lattice parameter for this composition.

Moreover, for slightly larger crystallites, this solubility limit may be pushed to a lower value of x. That is, for the x=0.12 sample calcined at 1250ºC, which has a crystallite size of 68 nm, the lattice parameter is slightly above the expected a_o value, although its error bar still touches the expected a_o dotted line. This small elevation with respect to the aforementioned line may signal a slight segregation of hafnia into a non-cubic phase. The lattice parameter increases because as hafnia segregates out of the cubic phase, the cubic structure becomes richer in Ce^{4+}, which has a radius of 0.97Å in 8-fold coordination, while that of Hf^{4+} is 0.78Å[32]. Notice that the lattice parameter of the 1050ºC sample with smaller crystallites but same x=0.12 composition is slightly below the expected cubic a_o line like that of the x=0.04 sample and thus less likely to have undergone hafnia segregation. Ultimately, the fact that the solubility limit for a 68 nm crystallite might be roughly 12% hafnia, while that of slightly smaller crystallites (i.e., 35-61 nm) is roughly 15% underscores the sensitivity of solubility to crystallite size in these submicron particles, and the importance of including the crystallite size when talking about the compositional domain in which these $(1-x)CeO_2$-$xHfO_2$ particles are cubic fluorite in structure.

The solubility limit determined in this study is consistent with the work of Chavan, et al[13]. The fact that this limit is lower than that found in other recent studies[17, 18] is largely attributable to differences in crystallite size. Thermodynamic research has revealed that the

enthalpy or Gibbs free energy of the monoclinic structure of pure hafnia is lower than that of the tetragonal or amorphous polymorphs when the surface/ interface areas are relatively low (large crystallite size), whereas at relatively high surface areas (small crystallite size), the amorphous or tetragonal polymorphs are energetically preferred[38]. (The energetics of the cubic hafnia structure were not considered in this article[38].) Therefore the findings of the study presented here help to provide a broader picture of how large ceria-hafnia crystallites can be and still maintain enhanced stability of the cubic structure relative to the stable phase diagram of ceria-hafnia[16]. That is, at a crystallite size of roughly 7 nm, the solubility limit for hafnia in the cubic fluorite structure with ceria is at least[17, 18] x=0.50, but when the crystallite size is closer to a tenth of a micron (i.e., 61 nm) as in this study, the solubility limit lies around 15% hafnia. It is also of interest to note that this limit is lower than the value determined for ceria-zirconia nanoparticles calcined at 1200°C and having roughly similar crystallite sizes[21]; for these (1-x)CeO_2-$x$$ZrO_2$ nanoparticles, tetragonal and monoclinic XRD peaks were absent from x=0 to at least x =0.30.

Another factor contributing to the limited solubility of hafnia in the cubic fluorite structure is the Ce^{3+} concentration. For the doped samples in Table 2, the fraction of Ce^{3+} (i.e., $Ce^{3+}/(Ce^{3+} + Ce^{4+})$) was found to be zero. In nanoparticulate studies of the twin system, ceria-zirconia, the concentration of Ce^{3+} was non-zero and helped to enhance the stability of the structurally cubic phase whether the nanoparticles were homogenized in an oxidizing or a reducing[22] environment. That is, a reduction of Ce^{4+} to larger Ce^{3+} ions could have helped to lessen the tensile stress created by the smaller Hf^{4+} ions and thus to stabilize the cubic fluorite structure. Similarly, even when the (1-x)CeO_2-$x$$HfO_2$ grains were micron-sized as in Gavrish, et al. (Table 1), reduction of cerium, as revealed by the grayish color of the powders, helped to stabilize the cubic structure to a x=0.425 hafnia content[19].

A final factor that may explain some of the differences in the compositional width of the pure cubic fluorite structure for the (1-x)CeO_2-$x$$HfO_2$ crystallites is preparation method. Zhou, et al.[18], prepared samples by a sol-gel method with calcination for 5 hours at 700°C while Baidya, et al.[17], relied on solution combustion with a dwell temperature of 1000°C for 30 to 40 seconds. These methods may have resulted in greater initial ceria-hafnia homogeneity and not required this study's high calcination temperatures that caused sample coarsening. Also, the co-precipitation/annealing method used here may have resulted in a non-negligible defect density, and the presence of defects can facilitate nucleation of the monoclinic structure from the tetragonal structure in zirconia[39], the twin of hafnia.

Also noteworthy is the possible appearance of a tetragonal phase in this study's nanostructured (1-x)CeO_2-$x$$HfO_2$ as the tetragonal structure is technically not stable at room temperature based on the *stable* lines in the phase diagram for ceria-hafnia[16] and is rarely cited in the literature on ceria-hafnia, except for the previously mentioned study on micron-sized powders, which were likely highly reduced based on the temperatures employed (>1500ºC) and grayish color[19]. The absence of the tetragonal structure in other studies with size data may be related to the crystallite size found in other studies, which was generally smaller[17, 18] or smaller and having a lower hafnia content[14] than the crystallites in this study. Furthermore, the greater intensity of the tetragonal phase (101) peak in the 0.73 HfO_2-0.27CeO_2 sample (Fig. 2a) than in the other samples calcined in air is due to the mid-value composition combined with small size of the crystallites (15 nm). The small size may be due a slight displacement from the center of the furnace during calcination as mentioned above.

5. Conclusions

Crystallites of (1-*x*)CeO_2-*x*HfO_2 were prepared by co-precipitation and subsequently calcined. The size of the crystallites varied from 140 nm for *x*=0 to 15 nm for *x*=0.73 based on the Scherrer equation. From *x* =0 to *x*=0.14, only cubic fluorite x-ray diffractions peaks are visible, and the lattice parameters are roughly consistent with structurally cubic solid solutions having these compositions, while non-cubic diffraction peaks can be seen in the *x*=0.26 sample. Therefore, the solubility limit of hafnia in a cubic fluorite structure with ceria, is roughly between *x*=0.14 and *x* = 0.26 for 61 nm to 40 nm crystallites, the crystallite sizes of the respective compositions. Calculations suggest that 15% hafnia remains in cubic fluorite solid solution with ceria for the *x* =0.26 sample and, as a very rough approximation, the *x*=0.73 sample, having 35 nm crystallites, shares this 15% limit. The latter composition, in addition to cubic and monoclinic peaks, shows a relatively strong peak consistent with the presence of a tetragonal structure, which is different than the bulk phase diagram for ceria-hafnia. The limited solubility of hafnia in ceria in this study, is due to the intermediate crystallite size relative to other studies and the roughly zero Ce^{3+} content based on XANES spectroscopy.

Acknowledgments

This work was supported by the NSF MRSEC Program under Award No. DMR-0213574, the DOE/BES-Hydrogen Fuel Initiative program (#DE-FG02-05ER15730), and New York State Office of Science**,** Technology and Academic Research (NYSTAR). SWC acknowledges the support from National Science Foundation-DMR 1206764. Use of the National Synchrotron Light Source, Brookhaven National Laboratory, was supported by the U.S. Department of Energy, Office of Science, Office of Basic Energy Sciences, under Contract No. DE-AC02-98CH10886.

List of Captions

Fig. 1: Determination of the minimum temperature for complete homogenization by plotting lattice parameter of 88%CeO_2-12HfO_2 crystallites as a function of maximum calcination temperature. The dotted horizontal line represents the expected lattice parameter for a structurally cubic sample of this composition. Note that the point corresponding to a temperature of 25°C is for an uncalcined sample and is included here for comparison.

Fig. 2: a) XRD of (1-x)CeO_2-xHfO_2 crystallites. The structures observed are pure cubic (c) from x =0 to x =.14 and predominantly cubic (c*) for x =0.26. For x>0.26, the monoclinic (m) and possibly the tetragonal structure (t) is also present to varying degrees. b) I.C.D.D. data for ceria, tetragonal hafnia, and monoclinic hafnia (reference numbers 00-034-0394, 04-002-5486, and 04-005-4477). (1-x)CeO_2-xHfO_2 crystallite peak positions will differ slightly from the ICDD data because the ceria-hafnia samples are solid solutions, not pure CeO_2 or HfO_2.

Fig. 3: XRD between 27° and 35° of (1-x)CeO_2-xHfO_2 crystallites annealed in air with a hold of 15 minutes at 1250°C.

Fig. 4: Lattice parameter as a function of x in $(1-x)CeO_2$-$xHfO_2$. The dotted line indicates the expected lattice parameters for cubic solid solutions of $(1-x)CeO_2$-$xHfO_2$ as contrasted to the actual experimental values for samples calcined at 1250ºC or 1050ºC.

Fig. 5: XANES spectra of $(1-x)CeO_2$ - $xHfO_2$ crystallites as at the Ce LIII absorption edge.

[1] N. Izu, T. Itoh, W. Shin, I. Matsubara, N. Murayama, The effect of hafnia doping on the resistance of ceria for use in resistive oxygen sensors, Sensors and Actuators B: Chemical, 123 (2007) 407-412. http://dx.doi.org/10.1016/j.snb.2006.09.001

[2] B.M. Reddy, P. Bharali, G. Thrimurthulu, P. Saikia, L. Katta, S.-E. Park, Catalytic Efficiency of Ceria-Zirconia and Ceria-Hafnia Nanocompoisites for Soot Oxidation, Catal. Lett., 123 (2008) 327-333. doi: 10.1007/s10562-008-9427-3

[3] T. Vinodkumar, D. Naga Durgasri, B.M. Reddy, Design of transition and rare earth metal doped ceria nanocomposite oxides for CO oxidation, Int. J. Adv. Eng. Sci. Appl. Math., 5 (2013) 224-231.

[4] P. Bharali, G. Thrimurthulu, L. Katta, B.M. Reddy, Preparation of highly dispersed and thermally stable nanosized cerium–hafnium solid solutions over silica surface: Structural and catalytic evaluation, J. Ind. Eng. Chem., 18 (2012) 1128-1135. http://dx.doi.org/10.1016/j.jiec.2012.01.017

[5] D.P. Brunco, A. Dimoulas, N. Boukos, M. Houssa, T. Conard, K. Martens, C. Zhao, F. Bellenger, M. Caymax, M. Meuris, M.M. Heyns, Materials and electrical characterization of molecular beam deposited CeO_2 and CeO_2/HfO_2 bilayers on germanium, J. Appl. Phys., 102 (2007) 024104-024101-024104-024108. doi: 10.1063/1.2756519

[6] M. Veszelei, L. Kullman, M.S. Mattsson, A. Azens, C.G. Granqvist, Optical and electrochemical properties of Li+ intercalated Zr-Ce oxide and Hf-Ce oxide films, J. Appl. Phys., 83 (1998) 1670-1676. doi: 10.1063/1.366883

[7] V.D. Kushkov, A.V. Mel'nikov, A.M. Zaslavskii, The synthesis of cerium hafnate and phase relationships in films of the HfO2-CeO2 system, Russian Journal of Inorganic Chemistry, 34 (1989) 1548-1549.

[8] F. Zhang, P. Wang, J. Koberstein, S. Khalid, S.-W. Chan, Cerium oxidation state in ceria nanoparticles studied with X-ray photoelectron spectroscopy and absorption near edge spectroscopy, Surf. Sci., 563 (2004) 74-82. doi: 10.1016/j.susc.2004.05.138

[9] N. Nakajima, H. Mitani, Y. Yamamura, T. Tsuji, Thermodynamic and mechanical properties of $Ce_{1-x}Hf_xO_2$ (x=0-0.10) solid solutions, Journal of Nuclear Materials, 294 (2001) 188-192. doi: 10.1016/S0022-3115(01)00456-1

[10] J.R. Scheffe, R. Jacot, G.R. Patzke, A. Steinfeld, Synthesis, Characterization, and Thermochemical Redox Perfomance of Hf^{4+}, Zr^{4+}, and Sc^{3+} Doped Ceria for Splitting CO2, J. Phys. Chem C, 117 (2013) 24104-24114.

[11] D. Harshini, D.H. Lee, J. Jeong, Y. Kim, S.W. Nam, H.C. Ham, J.H. Han, T.-H. Lim, C.W. Yoon, Enhanced oxygen storage capacity of $Ce_{0.65}Hf_{0.25}M_{0.1}O_{2-\delta}$ (M = rare earth elements): Applications to methane steam reforming with high coking resistance, Appl. Catal. B, 148-149 (2014) 415-423.

[12] E. Debray, P. Malou, B. Chappey, Influence du dioxyde de hafnium sur la conductivite electronique du dioxyde de cerium, Comptes Rendus des Seances de l'Academie des Sciences, Serie II (Mecanique-Physique, Chimie, Sciences de la Terre, Sciences de l'Universe), 296 (1983) 337-342.

[13] A.K. Tyagi, S.V. Chavan, Investigations on ceria-hafnia system for phase analysis, and HT-XRD studies on a few cubic compositions, Mater. Sci. Eng., A, 433 (2006) 203-207. doi: 10.1016/j.msea.2006.06.110

[14] B.M. Reddy, P. Bharali, P. Saikia, A. Khan, S. Loridant, M. Muhler, W. Grünert, Hafnium Doped Ceria Nanocomposite Oxide as a Novel Redox Additive for Three-Way Catalysts, J. Phys. Chem C, 111 (2007) 1878-1881. doi: 10.1021/jp068531i

[15] L. Passerini, Isomorfismo tra ossidi di metalli tetravalenti (Isostructuralism between the oxides of the tetravalent metals), Gaz. Chem. Ital. , 60 (1930) 762-776.

[16] H. Fujimori, M. Yashima, S. Sasaki, M. Kakihana, T. Mori, M. Tanaka, M. Yoshimura, Internal distortion in ceria-doped hafnia solid solutions: High-resolution X-ray diffraction and Raman scattering, Phys. Rev. B: Conden. Matter, 64 (2001) 134104/134101-134105 doi: 10.1103/PhysRevB.64.134104

[17] T. Baidya, M.S. Hegde, J. Gopalakrishnan, Oxygen-Release/Storage Properties of $Ce_{0.5}M_{0.5}O_2$ (M=Zr, Hf) Oxides: Interplay of Crystal Chemistry and Electronic Structure, J. Phys. Chem. B, 111 (2007) 5149-5154. doi: 10.1021/jp070525e

[18] G. Zhou, R. Gorte, Thermodynamic Investigation of the Redox Properties for Ceria-Hafnia, Ceria-Terbia, and Ceria-Praseodymia Solid Solutions, J. Phys. Chem B, 112 (2008) 9869-9875. doi: 10.1021/jp804089w

[19] A.M. Gavrish, E.I. Zoz, N.V. Gul'ko, A.E. Solov'eva, Solid Solutions in the System HfO_2-CeO_2, Inorganic Materials, 11 (1975) 574-576.

[20] J. Tang, F. Zhang, P. Zoogman, J. Fabbri, S.-W. Chan, Y. Zhu, L.E. Brus, M.L. Steigerwald, Martensitic phase transformation of isolated HfO_2, ZrO_2, and $Hf_xZr_{1-x}O_2$ ($0 < x < 1$) nanocrystals, Adv. Funct. Mater., 15 (2005) 1595-1602. doi: 10.1002/adfm.200500050

[21] F. Zhang, C.-H. Chen, J.C. Hanson, R.D. Robinson, I.P. Herman, S.-W. Chan, Phases in ceria-zirconia binary oxide (1-x)CeO_2-xZrO_2 nanoparticles: the effect of particle size, J. Am. Ceram. Soc., 89 (2006) 1028-1036. doi: 10.1111/j.1551-2916.2005.00788.x

[22] F. Zhang, C.-H. Chen, J.M. Raitano, J.C. Hanson, W.A. Caliebe, S. Khalid, S.-W. Chan, Phase stability in ceria-zirconia binary oxide nanoparticles: the effect of the Ce^{3+} concentration and the redox environment, J. Appl. Phys., 99 (2006) 84313/84311-84318. http://dx.doi.org/10.1063/1.2190712

[23] M. Bowden, ConvX computer software (1998).

[24] I. Coehlo, Koalariet for Win95 computer software (1997).

[25] B.D. Cullity, Elements of x-ray diffraction, second ed., Addison-Wesley, Reading, Massachusetts, 1978.

[26] D.-M. Smilgies, Scherrer grain-size analysis adapted to grazing-incidence scattering with area detectors, J Appl Crystallogr., 42 (2009) 1030–1034. doi: 10.1107/S0021889809040126

[27] J. Tang, J. Fabbri, R.D. Robinson, Y. Zhu, I.P. Herman, M.L. Steigerwald, L.E. Brus, Solid-Solution Nanoparticles: Use of a Nonhydrolytic Sol-Gel Synthesis to Prepare HfO_2

and $Hf_xZr_{1-x}O_2$ Nanocrystals, Chem. Mater., 16 (2004) 1336-1342. doi: 10.1107/S0021889809040126]

[28] A. Pramanick, S. Omar, J.C. Nino, J.L. Jones, Lattice parameter determination using a curved position-sensitive detector in reflection geometry and application to $Sm_{x/2}Nd_{x/2}Ce_{1-x}O_{2-d}$ ceramics, J. Appl. Crystallogr., 42 (2009) 490-495.

[29] M.U. Cohen, Rev. Sci. Instrum., 6 (1935).

[30] M.U. Cohen, Rev. Sci. Instrum., 7 (1936).

[31] D.-J. Kim, Lattice Parameters, Ionic Conductivies, and Solubility Limits in Fluorite-Structure MO2 Oxide (M=Hf^{4+}, Zr^{4+}, Ce^{4+}, Th^{4+}, U^{4+}), Journal of the American Ceramic Society, 72 (1989) 1415-1421.

[32] R.D. Shannon, Revised Effective Ionic Radii and Systematic Studies of Interatomic Distances in Halides and Chalcogenides, Acta Crystallographica, A32 (1976) 751-767.

[33] B. Ravel, M. Newville, ATHENA and ARTEMIS: interactive graphical data analysis using IFEFFIT Phys. Scr., 2005 (2005). doi: 10.1238/Physica.Topical.115a01007

[34] ICDD (2007). PDF 2007 (Database), edited by Dr. Soorya Kabekkodu, International Centre for Diffraction Data, Newtown Square, PA, USA. .

[35] ICDD (2009). PDF 2009 (Database), edited by Dr. Soorya Kabekkodu, International Centre for Diffraction Data, Newtown Square, PA, USA. .

[36] A.J. Allen, V.A. Hackley, P.R. Jemian, J. Ilavsky, J.M. Raitano, S.-W. Chan, In situ ultra-small-angle X-ray scattering study of the solution-mediated formation and growth of nanocrystalline ceria, J. Appl. Cryst., 41 (2008) 918-929. doi: 10.1107/S0021889808023078

[37] C.-K. Loong, M. Ozawa, The role of rare earth dopants in nanophase zirconia catalysts for automotive emission control, Journal of Alloys and Compounds, 303-304 (2000) 60-65. doi: 10.1016/S0925-8388(00)00607-1

[38] S.V. Ushakov, A. Navrotsky, Y. Yang, S. Stemmer, K. Kukli, M. Ritala, M.A. Leskela, P. Fejes, A. Demkov, C. Wang, B.-Y. Nguyen, D. Triyoso, P. Tobin, Crystallization in hafnia- and zirconia-based systems, Phys. Stat. Sol. (b), 241 (2004) 2268-2278. doi: 10.1002/pssb.200404935

[39] I.-W. Chen, Y.-H. Chaio, Martensitic nucleation in ZrO2, Acta Metall., 31 (1983) 1627-1638.

Figure 1

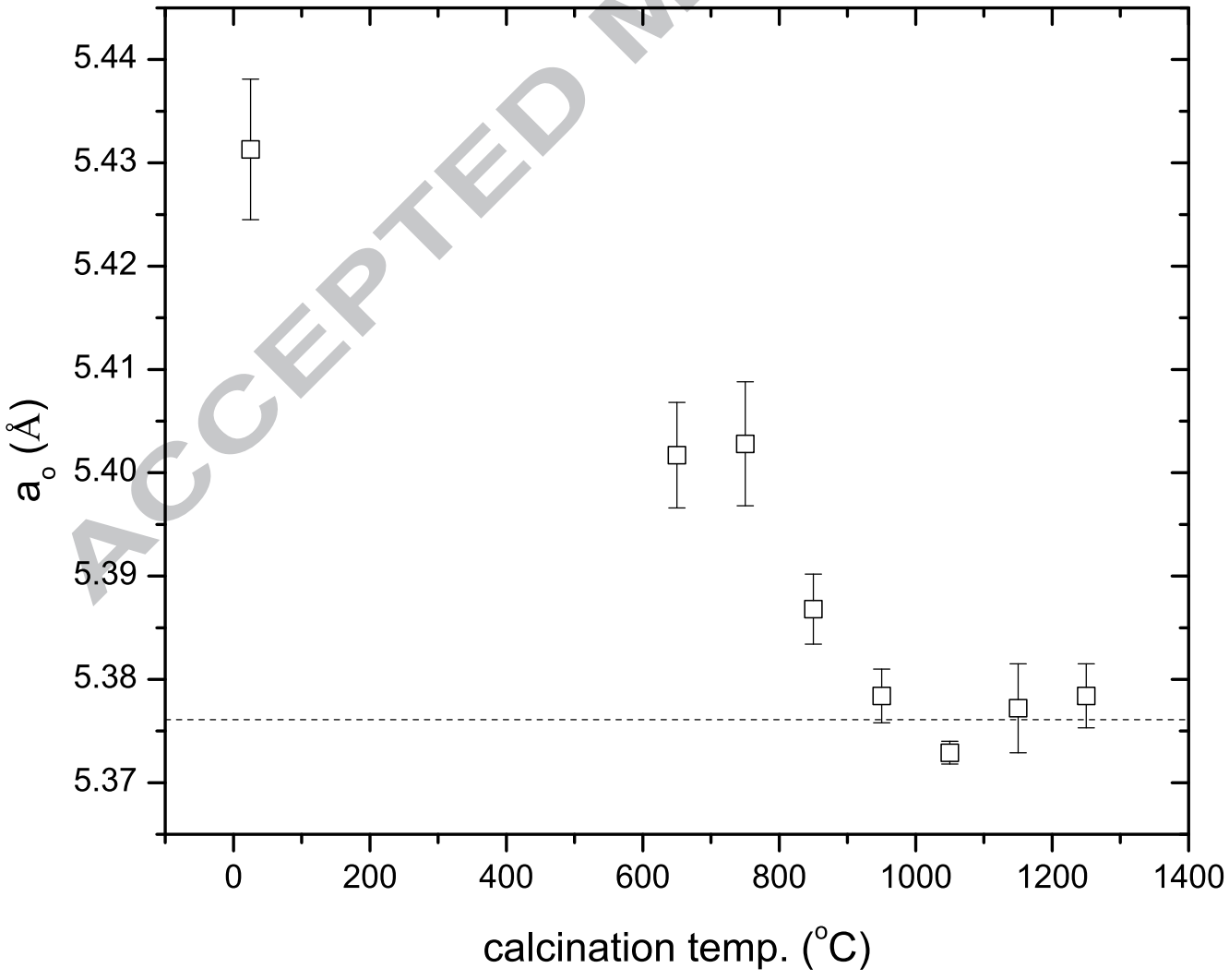

Figure 2a

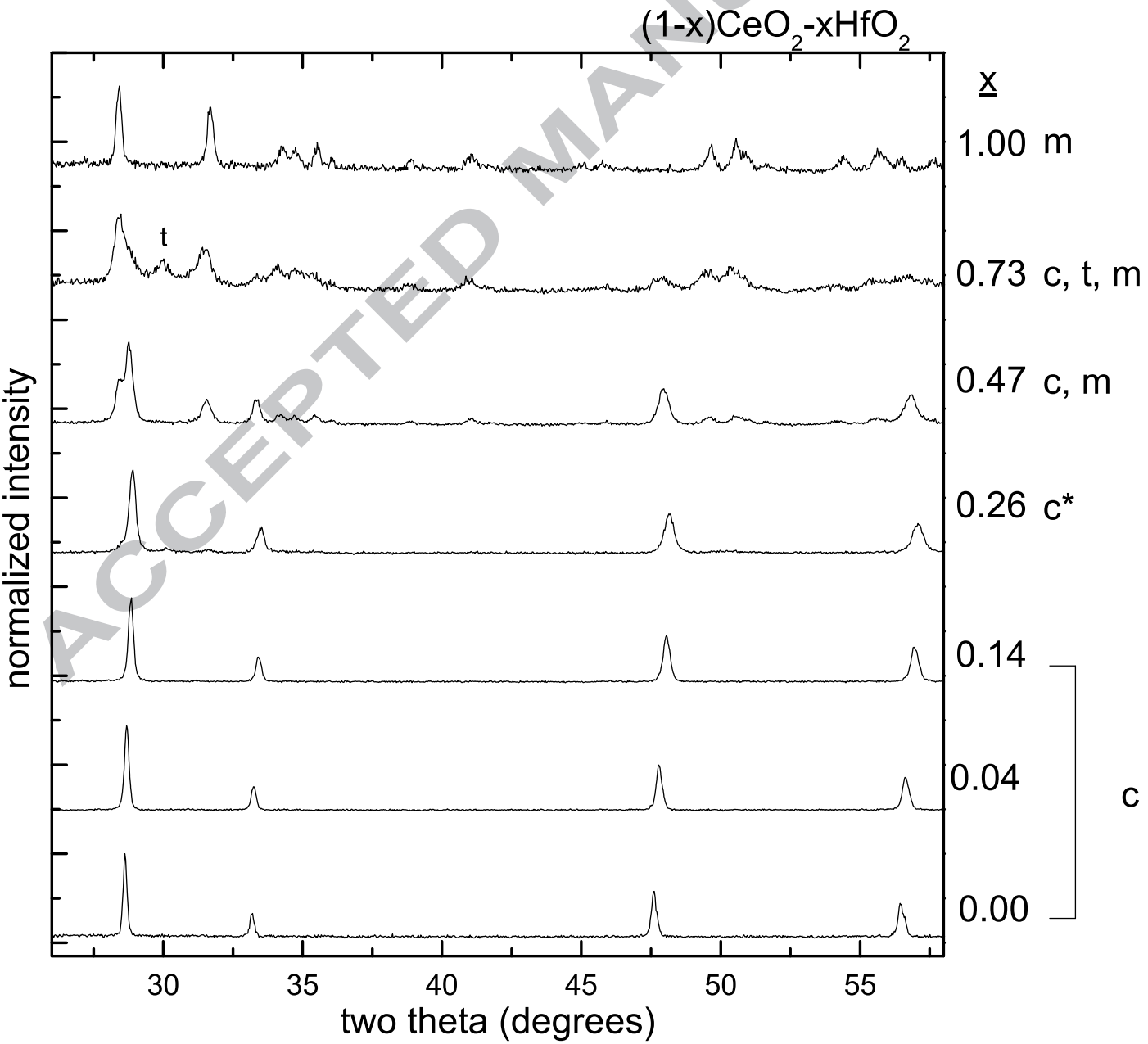

Figure 2b

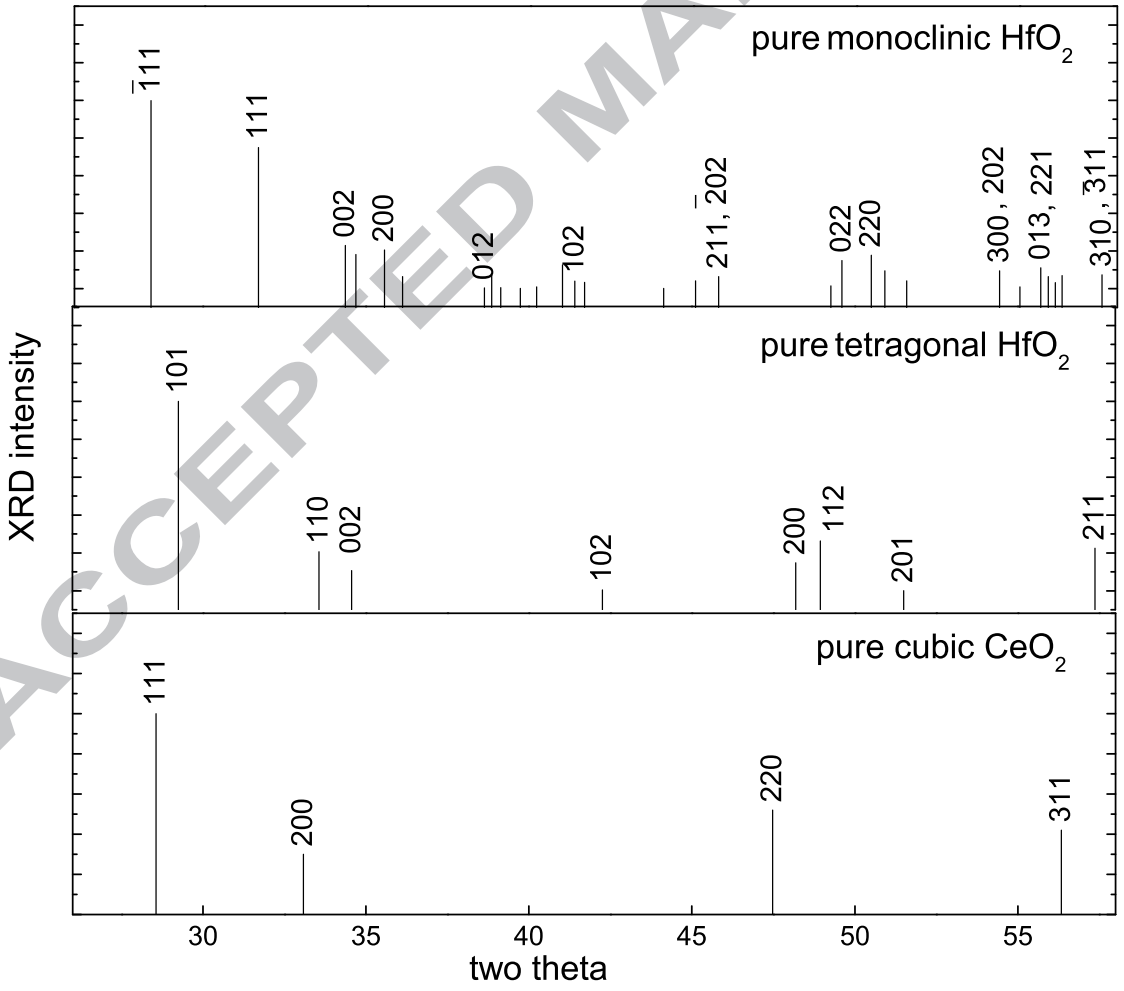

Figure 3

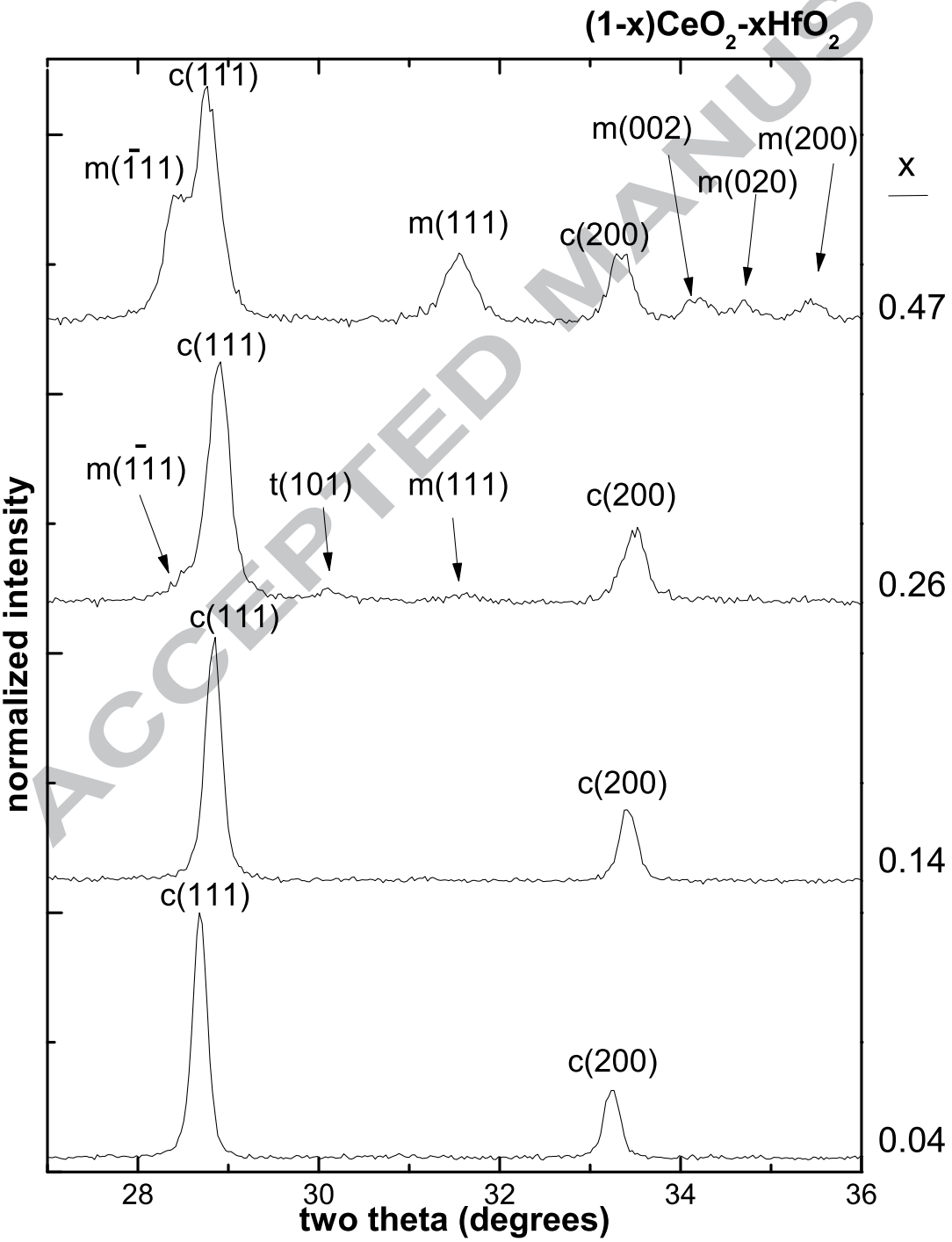

Figure 4

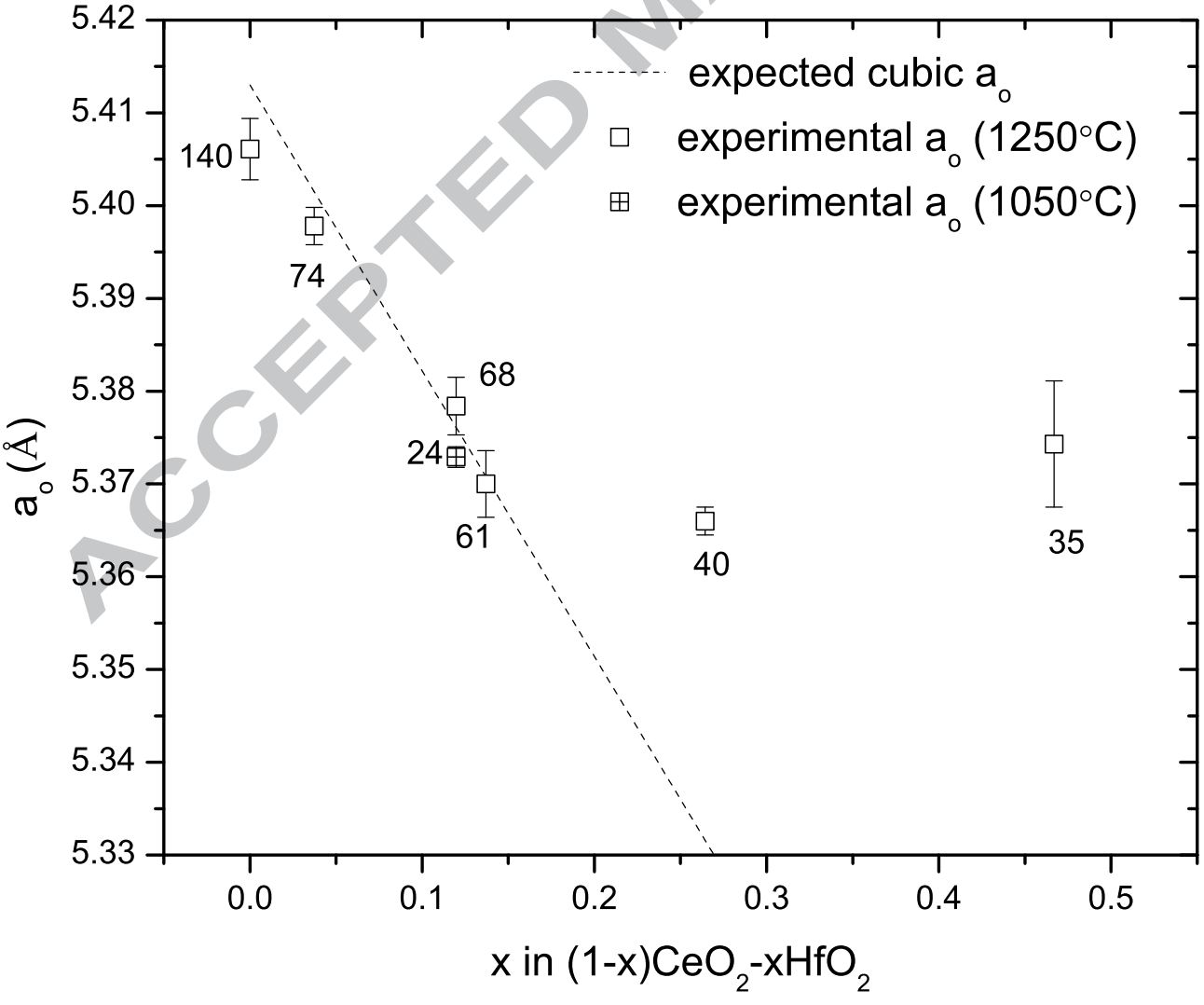

Figure 5

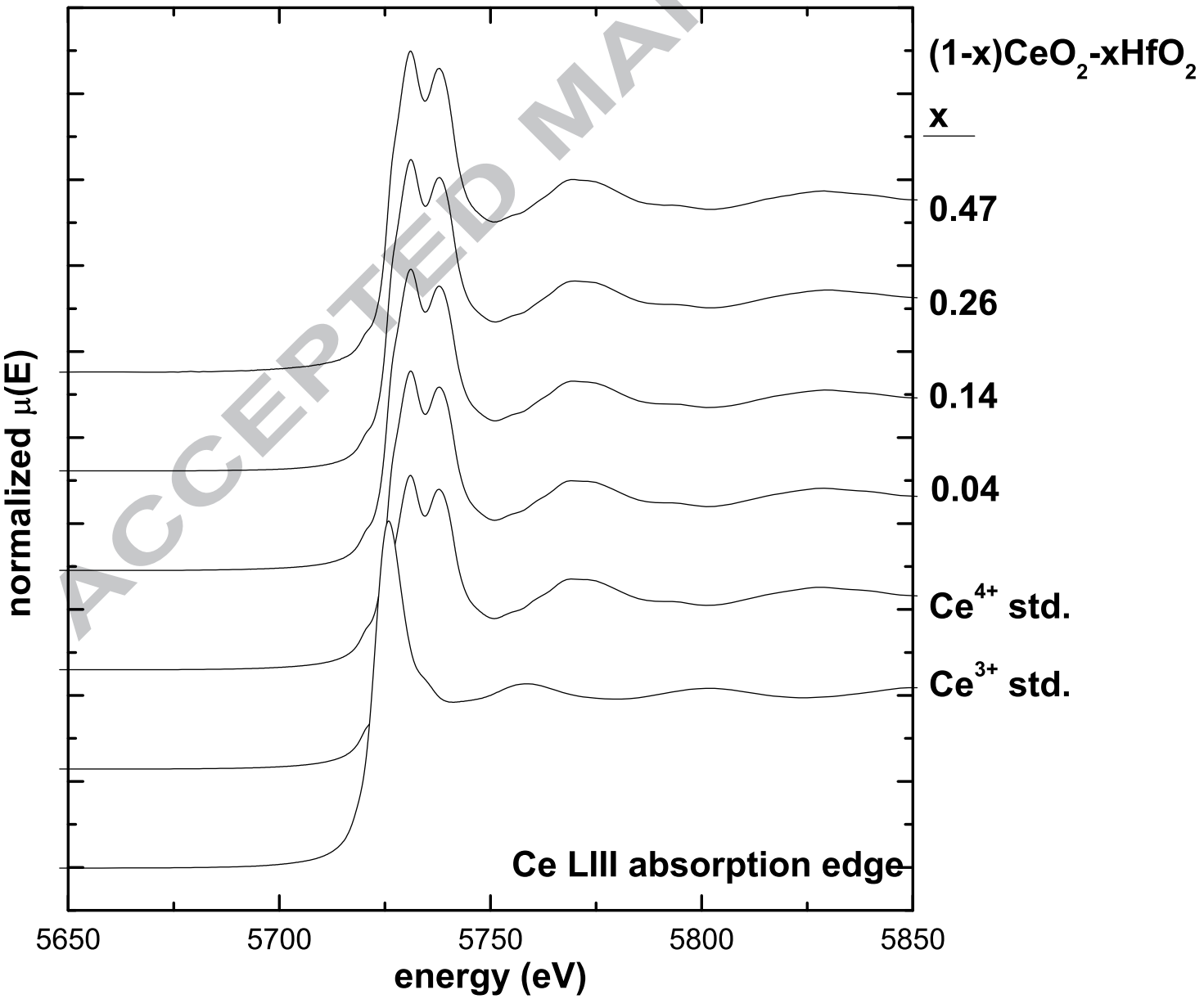

Highlights

- (1-x)CeO_2-xHfO_2 was precipitated (0<x<1) and calcined in air.
- For x≤0.14, crystallites ≤140 nm in size exhibit only the fluorite structure.
- This low hafnia solubility is attributable to no auto-reduction (Ce^{3+}=0).
- The low solubility is also due to the high temperature required for homogenization.
- Coarsening is lessened as Hf^{4+} ions slow cation diffusion in these crystallites.